Gravitational Waves with Pulsar Timing Arrays

Journée GPhys 2015

Antoine Lassus

Max-Planck-Institut für Radioastronomie

EPTA

- Introduction
- Pulsar Timing
- Gravitational Waves Signals & Detection
- Results from the EPTA dataset 2015

Introduction

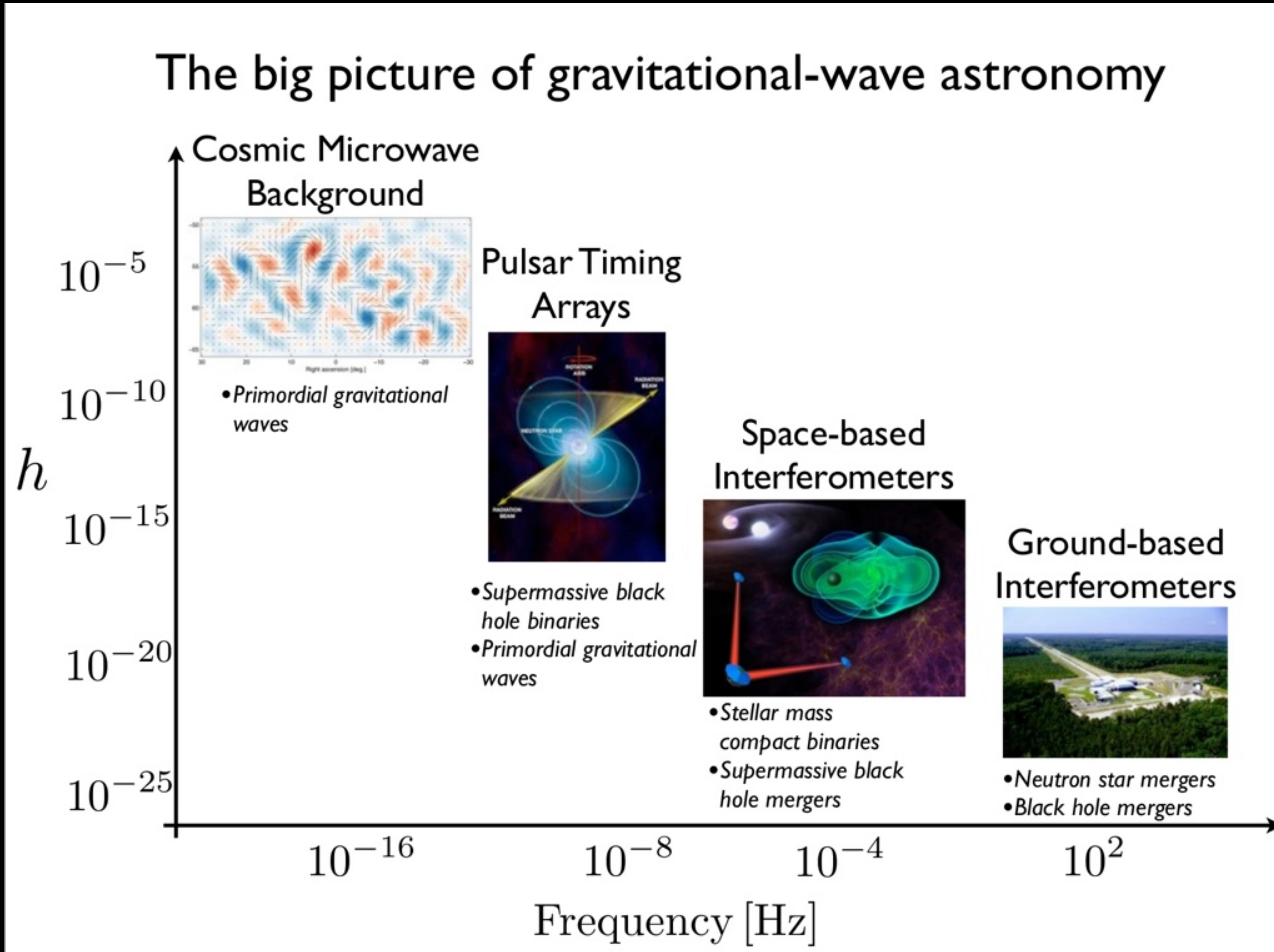

McLaughlin (2014)

Introduction

Concept :
Using pulsars
as galactic
scale
interferometer

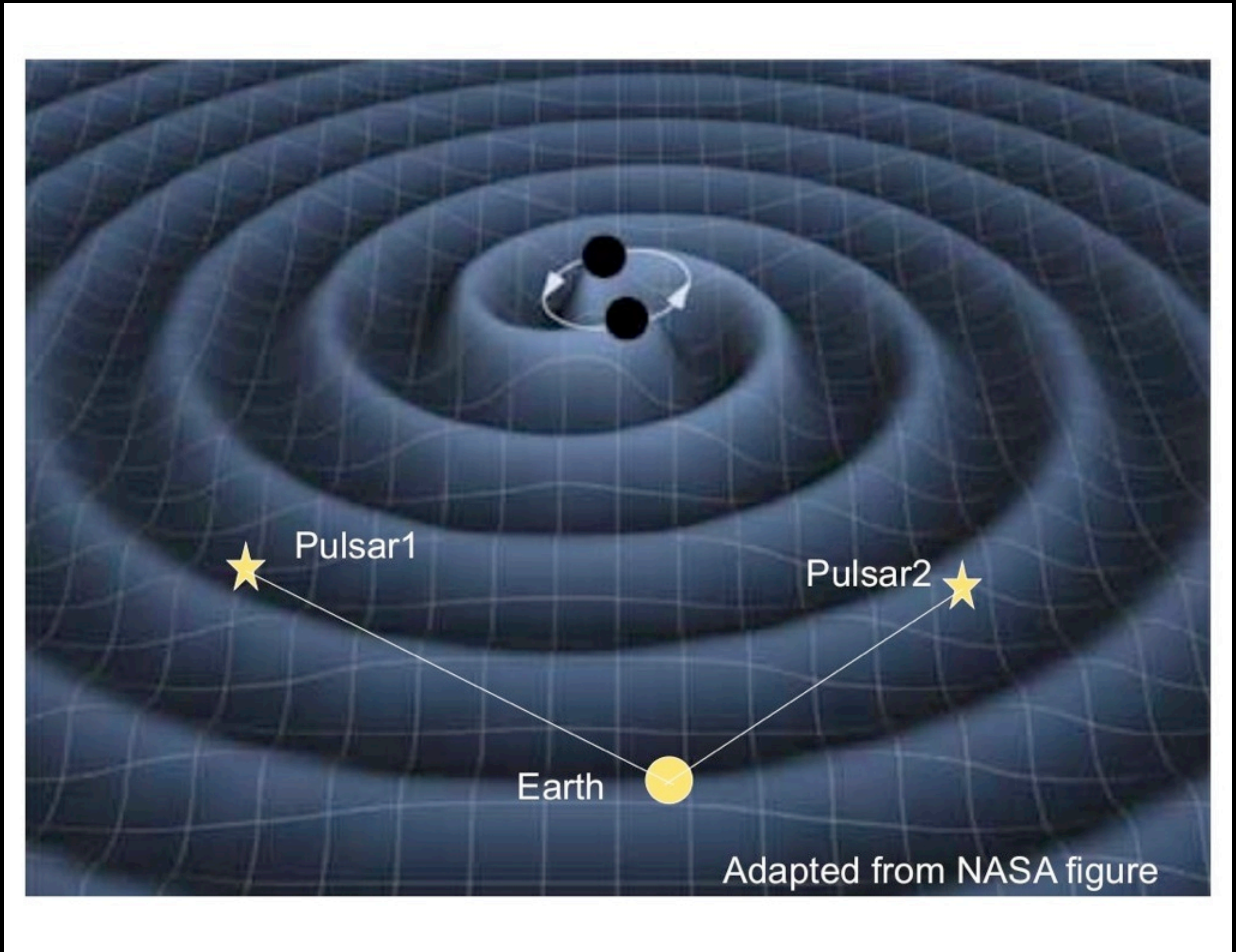

arms length ~ 100 pc -1 kpc

Pulsar Timing

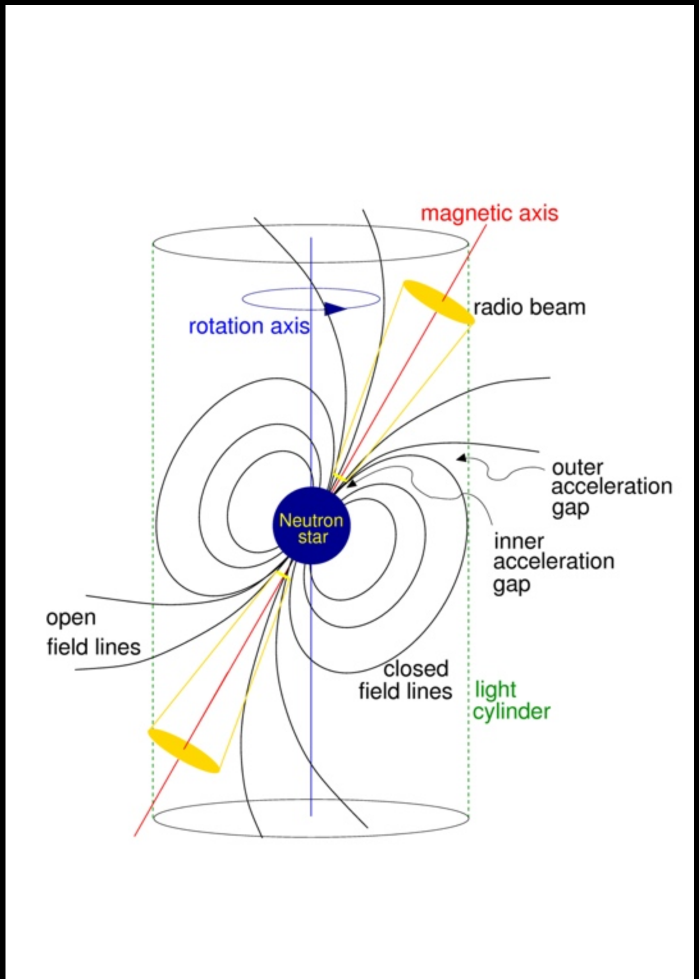

Highly magnetized, fast rotating neutron stars

$$1.3\mathrm{M}_{\odot} < M < 2.1\mathrm{M}_{\odot}$$

$$10^{10}\mathrm{G} < B < 10^{13}\mathrm{G}$$

$$1.4\mathrm{ms} < P < 12\mathrm{s}$$

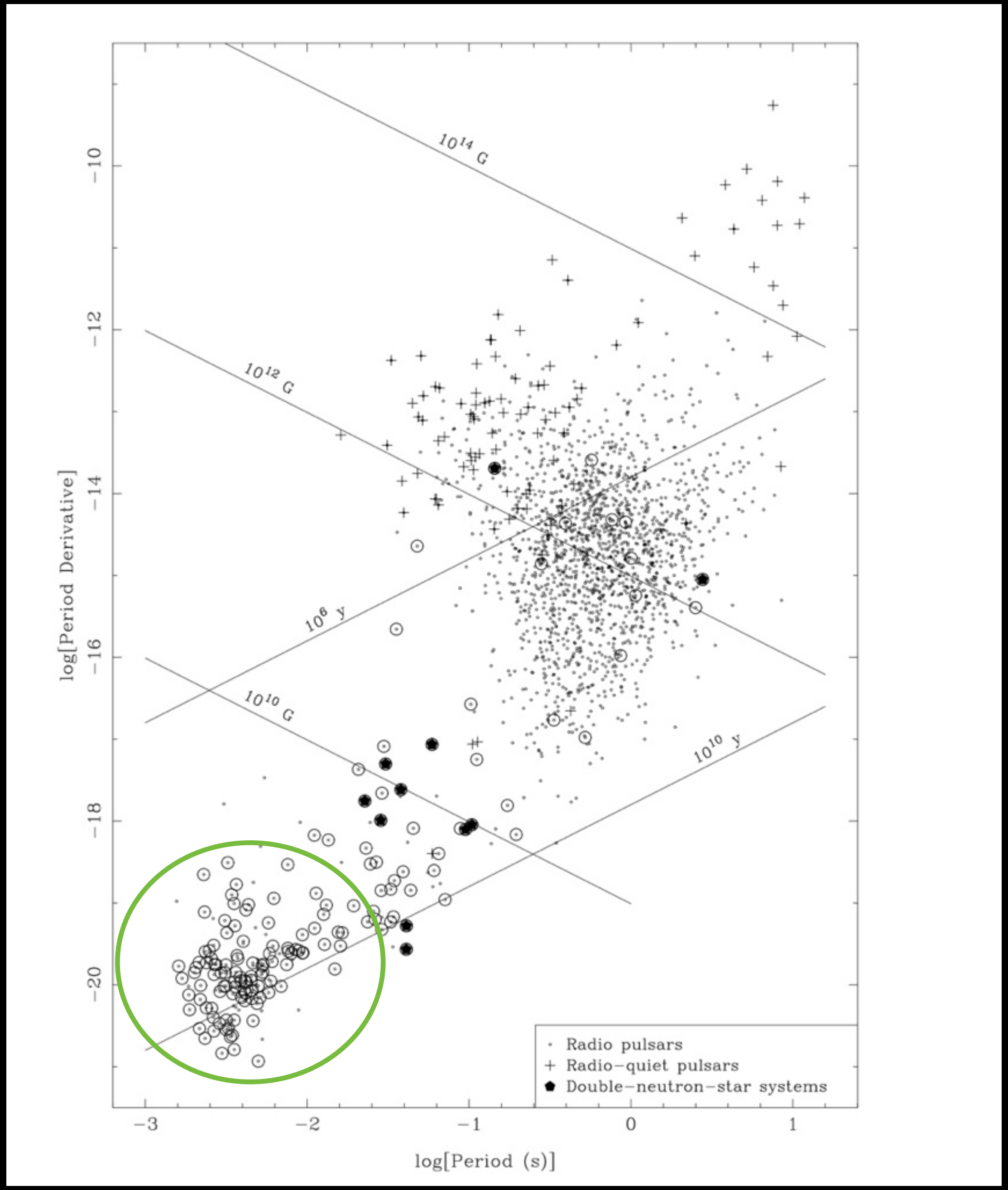

«Lighthouse effect» : sweeping radio beams as the pulsar rotates

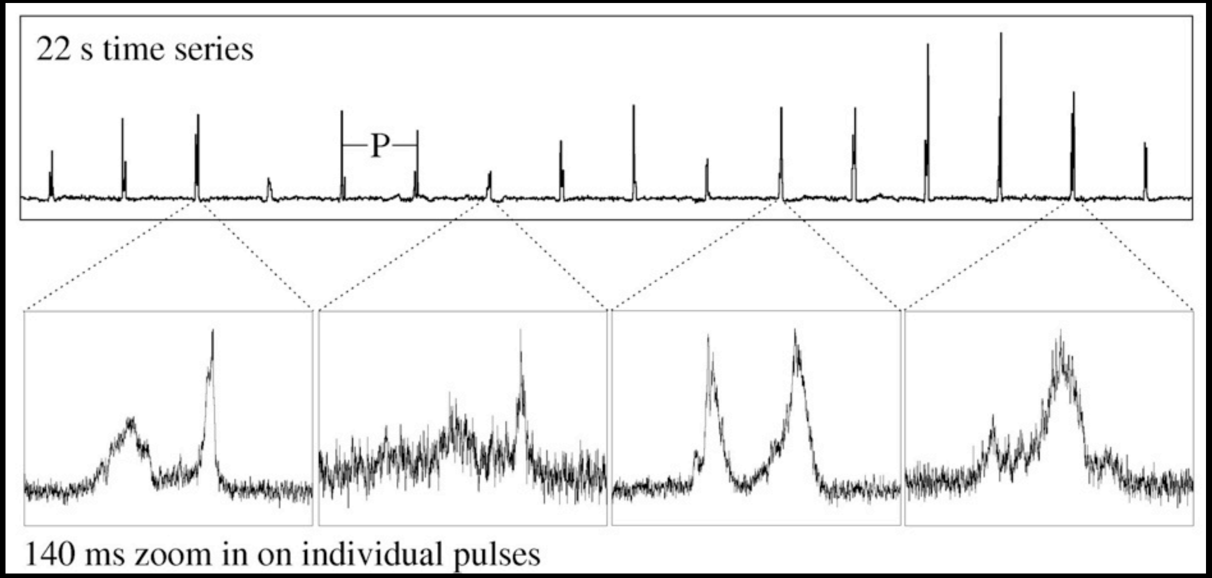

Millisecond Pulsars : recycled pulsars

$$1.4\mathrm{ms} < P < 30\mathrm{ms}$$

$$\dot{P} \sim 10^{-20}\mathrm{s.s}^{-1}$$

Pulsar Timing

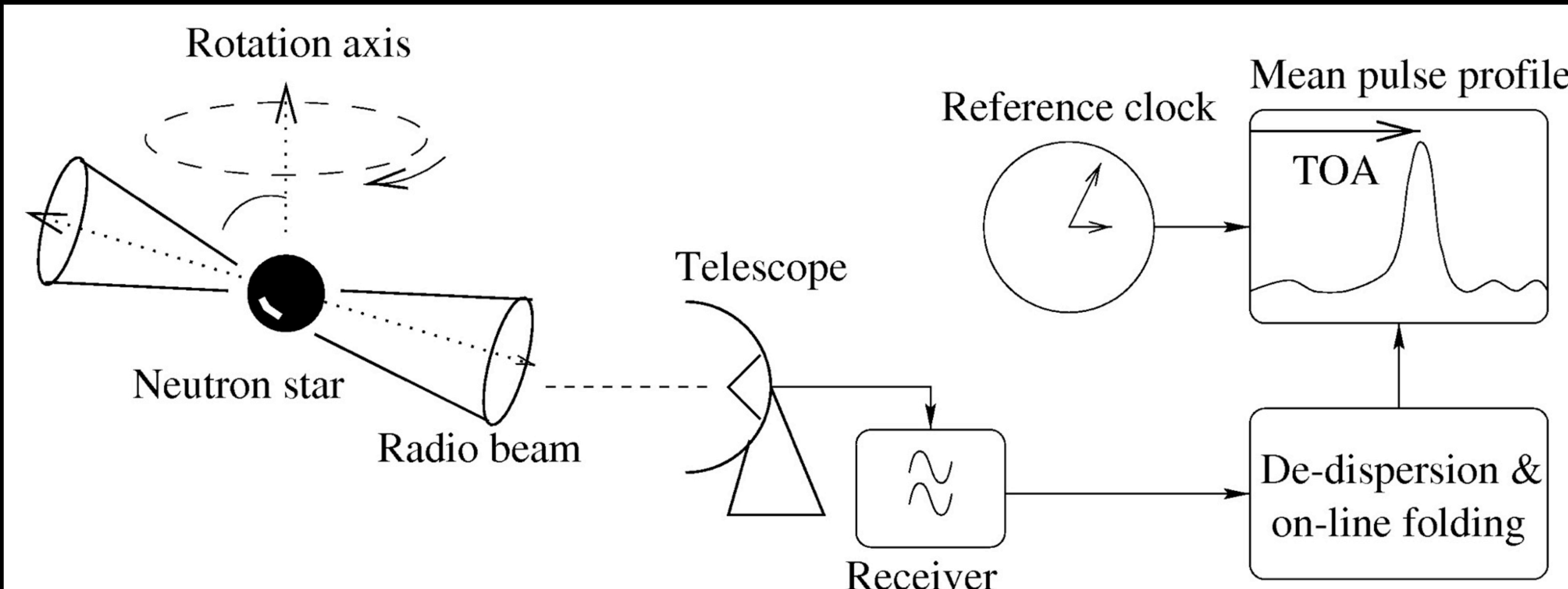

Kramer & Lorimer (2002)

$$\sigma_{TOA} \sim \frac{w}{SNR} \propto \frac{w}{S_{PSR}} \frac{T_{sys}}{A} \frac{1}{\sqrt{BT}}$$

$$r = TOA_{obs} - TOA_{mod}$$

Precision on TOAs as low as 30 ns

Minimizing the difference between Toas observed and predicted leads to construction of the timing model

Pulsar Timing

Timing Model :
- Period and period derivative (spin-down rate)
- Sky position, proper motion
- Dispersion measure due to the ISM (free electron density)
- Distance (parallax)
- Binary parameters:
  - Pulsar mass and companion mass (shapiro delay)
  - Keplerian parameters :
    - semi major axis
    - inclination
    - eccentricity
    - orbital period
  - Post-Keplerian parameters:
    - precession
    - orbital period derivative
    - geodetic precession
    - periastron advance
    - gravitational redshift

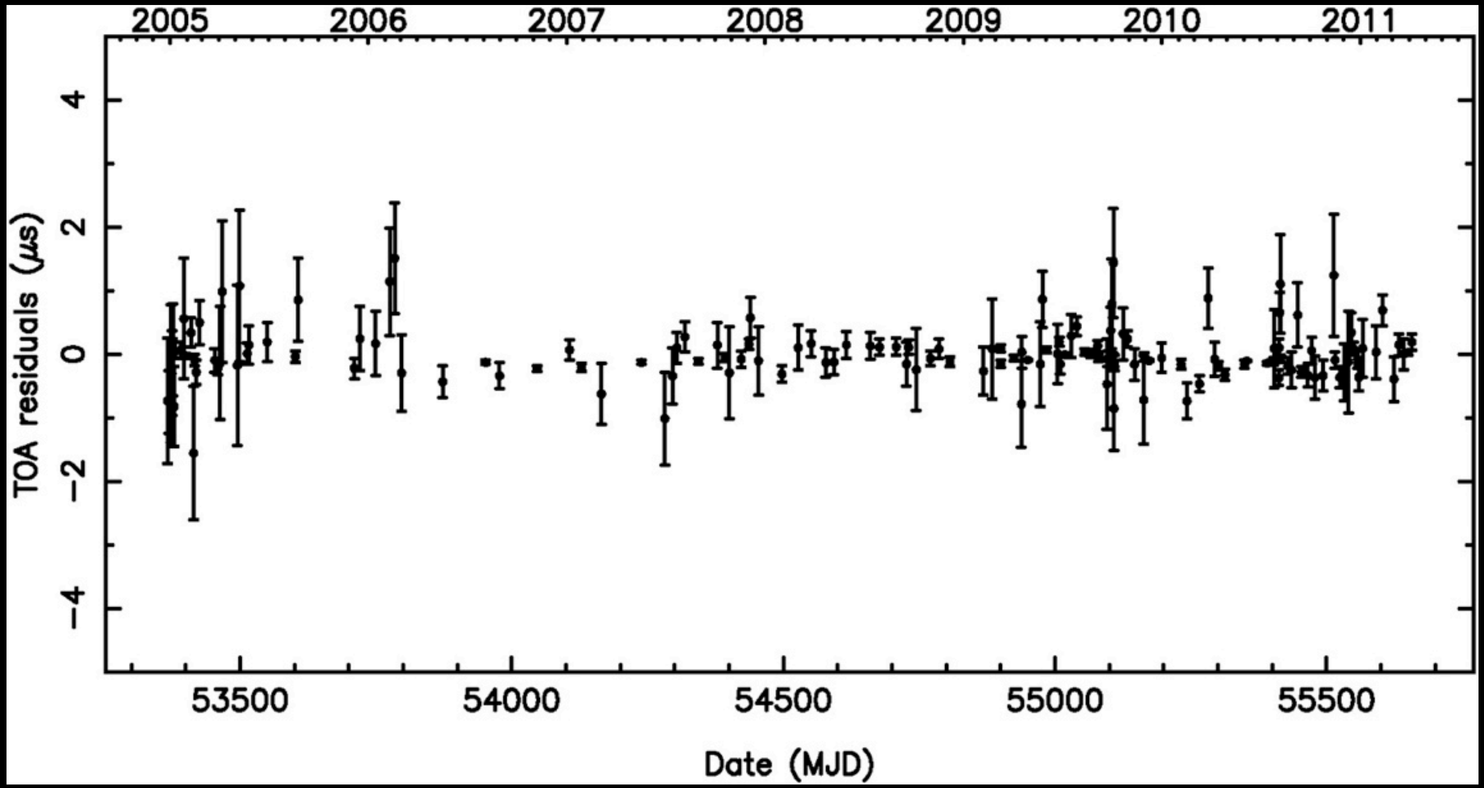

Residuals for the pulsar J1909-3744 with best fit rms of 110 ns

Pulsar Timing

Testing General Relativity

Double Pulsar J0737-3039

«Agreement with General Relativity within an uncertainty of 0.05%»

Kramer et al., Science 314, 97 (2006)

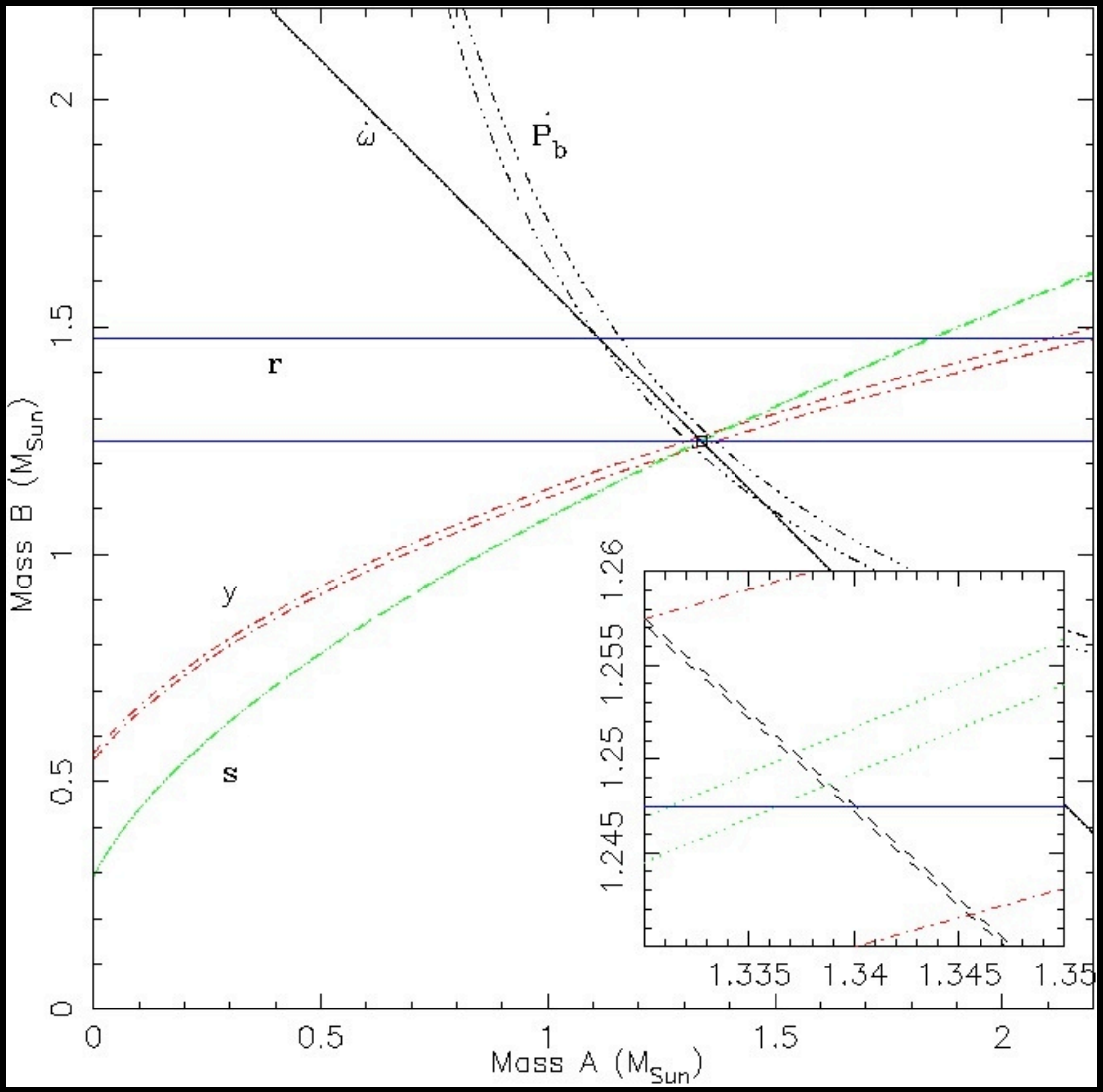

Constraining Alternate Theory

Scalar-Tensor Theories

From high asymetric WD-PSR binary

Freire et al., MNRAS 423, 3328 (2012)

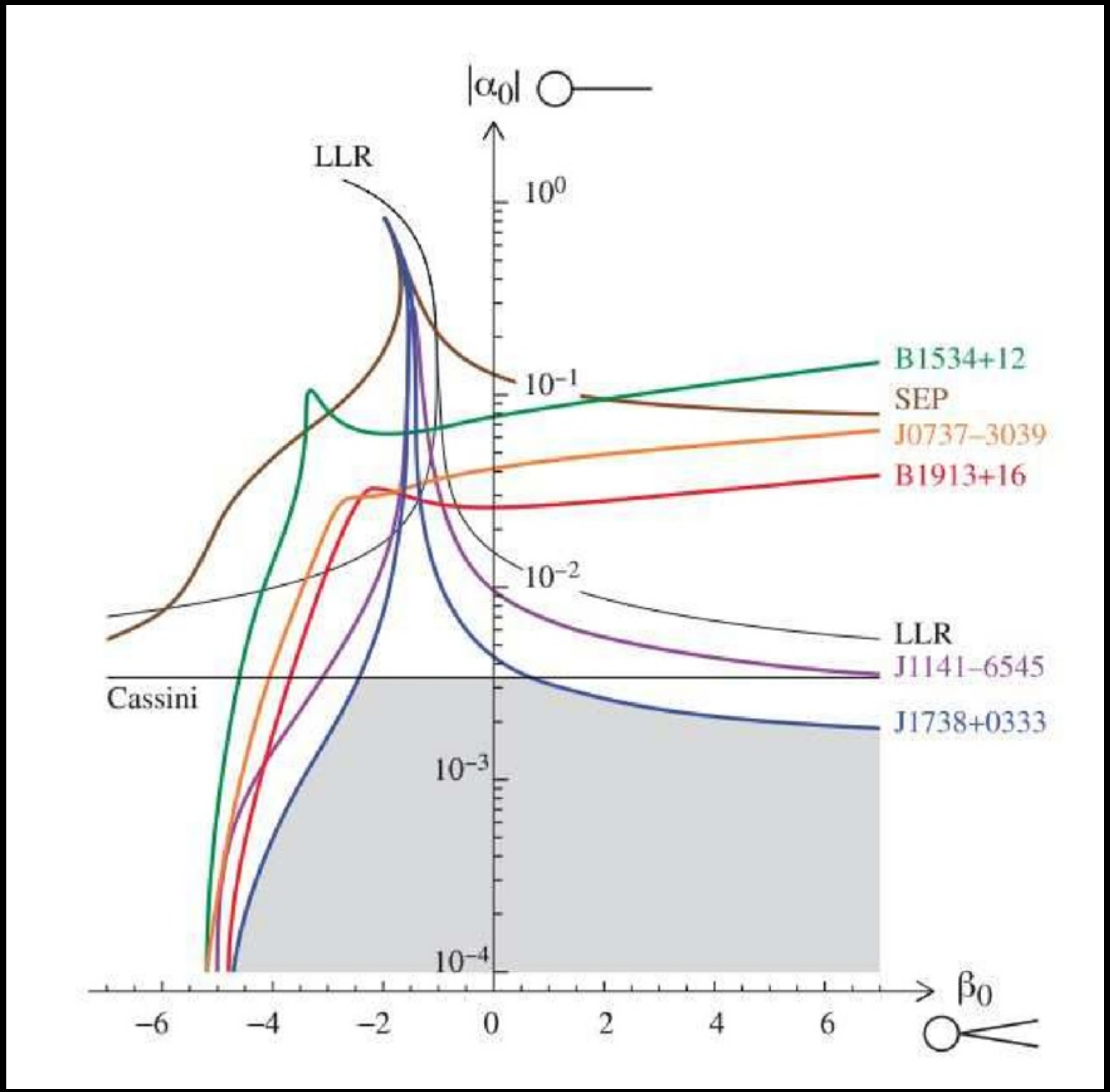

Pulsar Timing

Testing General Relativity

Gravitational Waves
Indirect detection
(Physics Nobel Prize 1993)

«Hulse-Taylor» Pulsar B1913+16

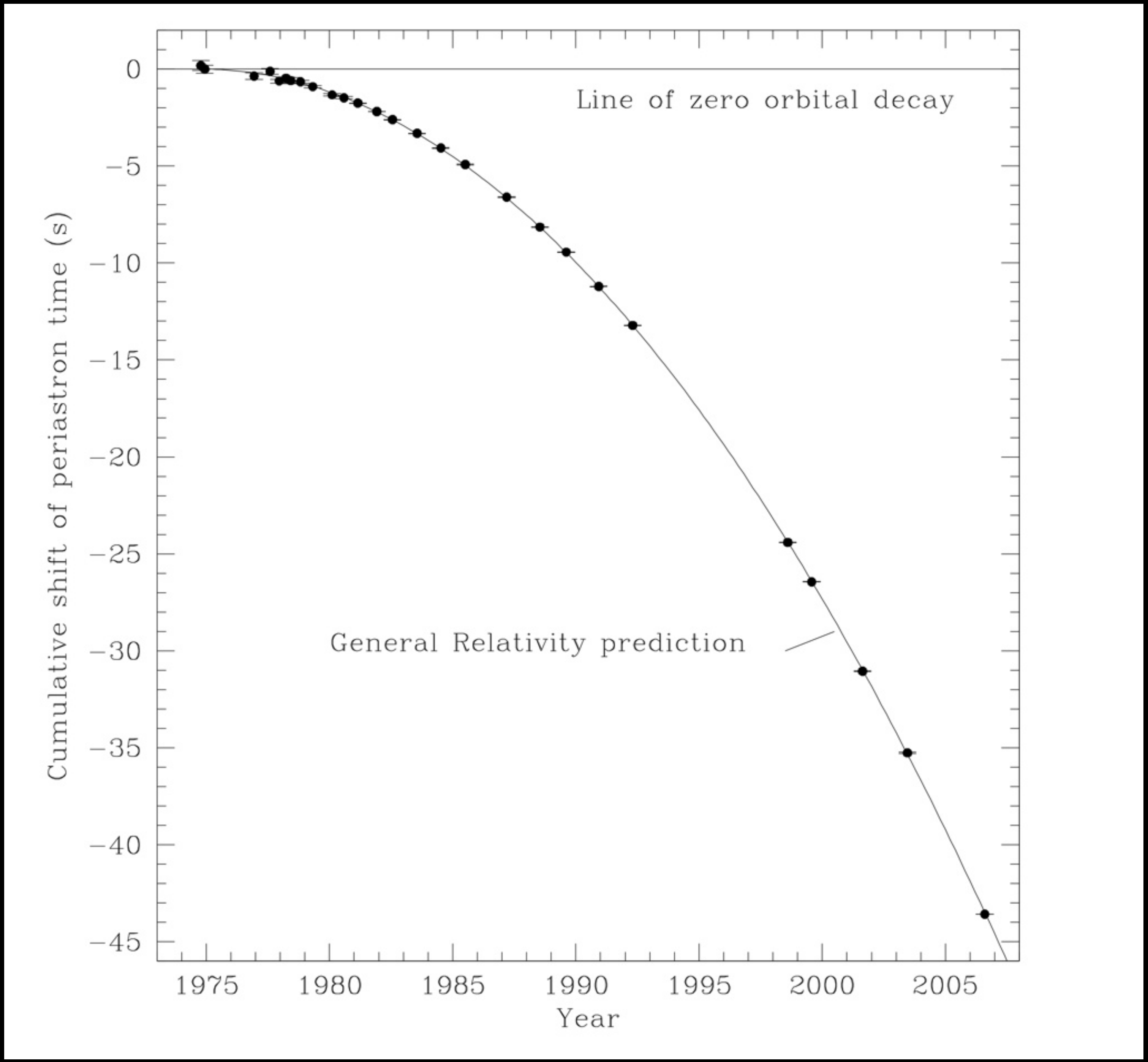

Gravitational Waves Signals & Detection

The gravitational wave modifies the path of the radio electromagnetic waves emitted by the pulsar inducing a modification of the observed frequency of the Toas.

$$r(t) = \int_0^t \frac{\nu(t') - \nu_0}{\nu_0} dt'$$

$$\frac{\nu(t) - \nu_0}{\nu_0} = \frac{1}{2} \frac{\hat{n}^i_\alpha \hat{n}^j_\alpha}{1 + \hat{n}_\alpha \cdot \hat{k}} \Delta h_{ij}$$

$$\Delta h_{ij} = h_{ij}(t_p) - h_{ij}(t)$$

Correlated signal between the pulsars of the array when observed from Earth

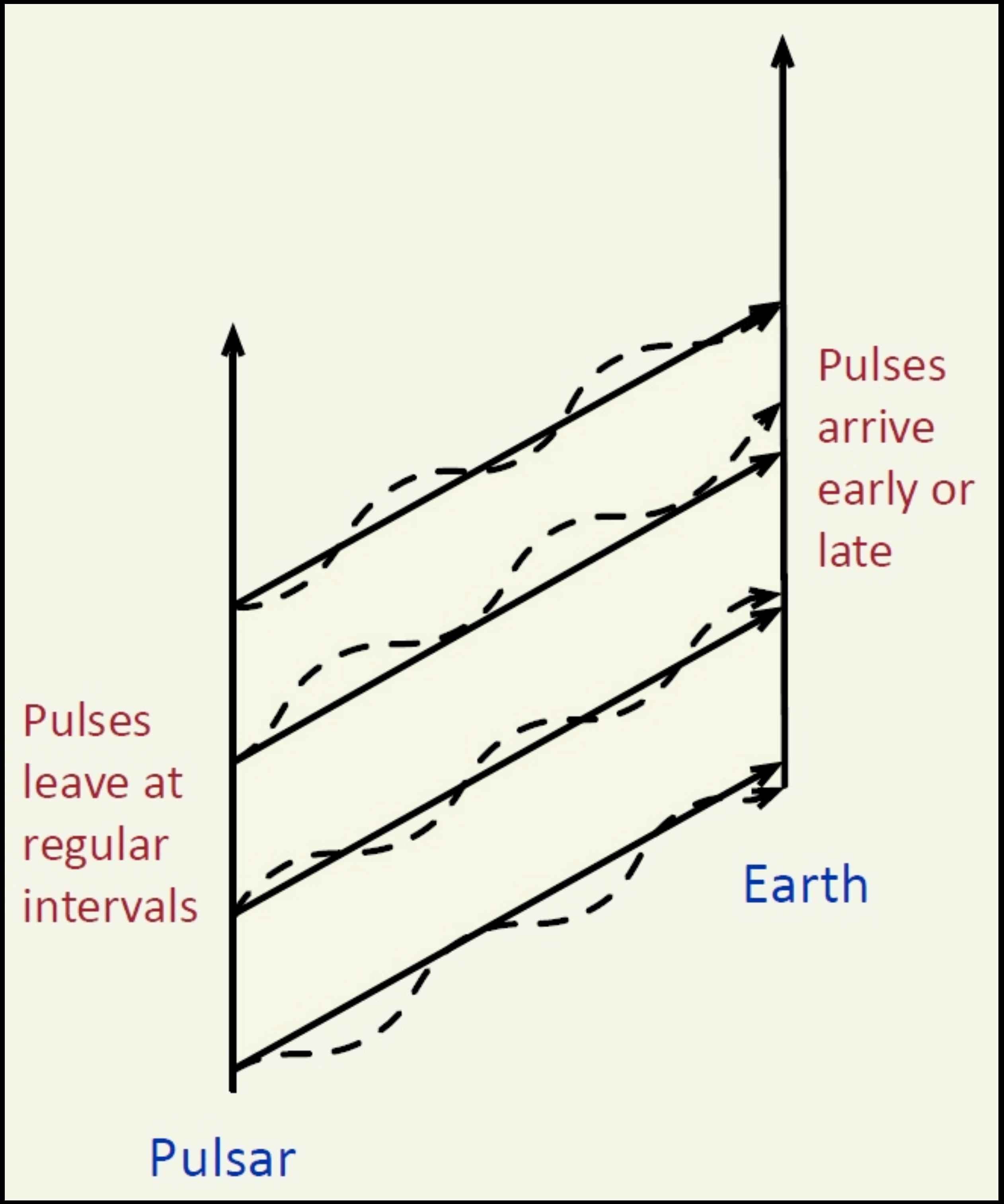

Gravitational Waves Signals & Detection

Expected signal in the nanoHertz regime from Super-Massive Black Holes Binaries

- Isotropic or Anisotropic stochastic GW background from a collection of sources

$$h_c(f) = A\left(\frac{f}{f_0}\right)^{-2/3}$$

- Monochromatic signal from distinguishable single sources above the background

$$\Delta h_{ij} = h_{ij}(t_p) - h_{ij}(t)$$

$$\begin{aligned} h_+(t) &= A(1+\cos^2 i)\cos(2\pi f t + \phi_0) \\ h_\times(t) &= -2A\cos i \sin(2\pi f t + \phi_0) \end{aligned}$$

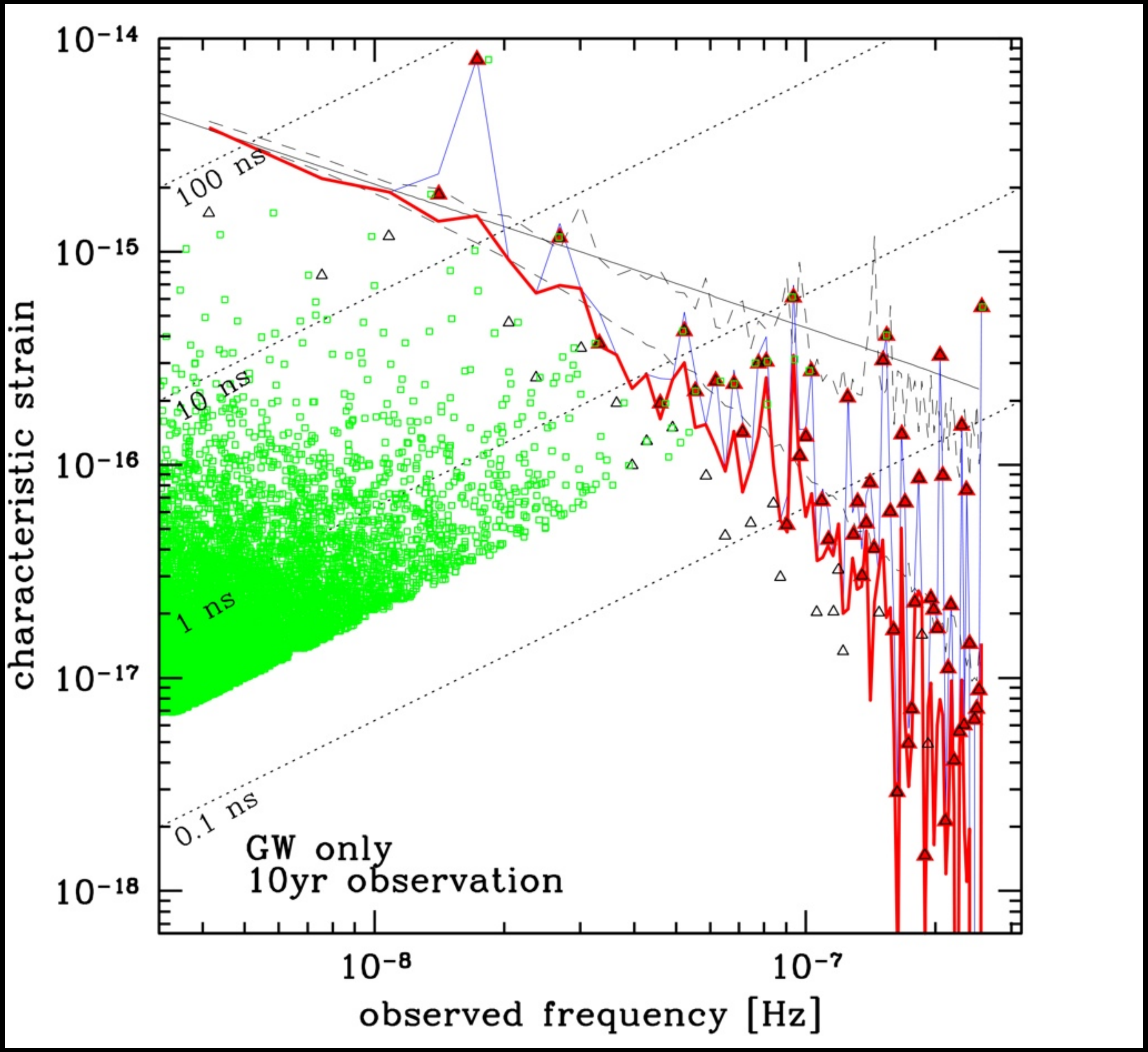

Sesana (2010)

Results from the EPTA dataset 2015

The European Pulsar Timing Array

Jodrell Bank (UK), 74m
Westerbork (Neartherland), 93m (eff)
Nançay (France), 94m (eff)
Effelsberg (Germany), 100m
SRT (Sardinia, Italy), 64m

LEAP : simultaneous observations
from all observatories
194m equivalent dish



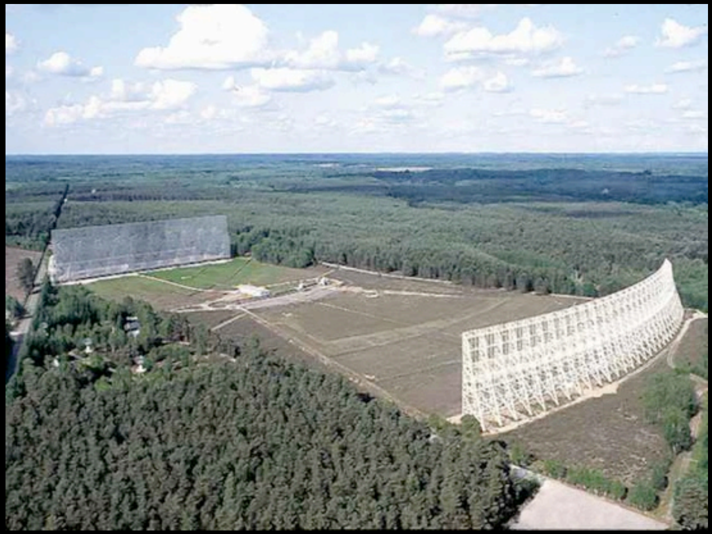

Results from the EPTA dataset 2015

2015 Dataset of 42 MSPs
(Desvignes & EPTA collaboration in prep.)

PSR JName	Observatories	N_{TOA}	T_{span} (yr)	RMS (μs)	Period (ms)	P_{orb} (d)
J0030+0451	eff, jbo, nrt	907	15.1	4.1	4.9	—
J0034−0534	nrt, wsrt	276	13.5	4.0	1.9	1.59
J0218+4232	eff, jbo, nrt, wsrt	1196	17.6	7.4	2.3	2.03
J0610−2100	jbo, nrt	1034	6.9	4.9	3.9	0.29
J0613−0200	eff, jbo, nrt, wsrt	1369	16.1	1.8	3.1	1.20
J0621+1002	eff, jbo, nrt, wsrt	673	11.8	15.6	28.9	8.32
J0751+1807	eff, jbo, nrt, wsrt	796	17.6	2.4	3.5	0.26
J0900−3144	jbo, nrt	875	6.9	3.1	11.1	18.74
J1012+5307	eff, jbo, nrt, wsrt	1459	16.8	1.6	5.3	0.60
J1022+1001	eff, jbo, nrt, wsrt	908	17.5	2.5	16.5	7.81
J1024−0719	eff, jbo, nrt, wsrt	561	17.3	1.7	5.2	—
J1455−3330	jbo, nrt	524	9.2	2.7	8.0	76.17
J1600−3053	jbo, nrt	531	7.7	0.46	3.6	14.35
J1640+2224	eff, jbo, nrt, wsrt	595	17.3	1.8	3.2	175.46
J1643−1224	eff, jbo, nrt, wsrt	759	17.3	1.7	4.6	147.02
J1713+0747	eff, jbo, nrt, wsrt	1188	17.7	0.68	4.6	67.83
J1721−2457	nrt, wsrt	150	12.8	11.7	3.5	—
J1730−2304	eff, jbo, nrt	285	16.7	3.9	8.1	—
J1738+0333	jbo, nrt	318	7.3	3.0	5.9	0.35
J1744−1134	eff, jbo, nrt, wsrt	536	17.3	0.86	4.1	—
J1751−2857	jbo, nrt	144	8.3	3.0	3.9	110.75
J1801−1417	jbo, nrt	126	7.1	2.6	3.6	—
J1802−2124	jbo, nrt	522	7.2	2.7	12.6	0.70
J1804−2717	jbo, nrt	116	8.4	3.1	9.3	11.13
J1843−1113	jbo, nrt, wsrt	224	10.1	0.71	1.8	—
J1853+1303	jbo, nrt	101	8.4	1.6	4.1	115.65
J1857+0943	eff, jbo, nrt, wsrt	444	17.3	1.7	5.4	12.33
J1909−3744	nrt	425	9.4	0.13	2.9	1.53
J1910+1256	jbo, nrt	112	8.5	1.9	5.0	58.47
J1911+1347	jbo, nrt	140	7.5	1.4	4.6	—
J1911−1114	jbo, nrt	130	8.8	4.8	3.6	2.72
J1918−0642	jbo, nrt, wsrt	278	12.8	3.0	7.6	10.91
J1939+2134	eff, jbo, nrt, wsrt	3174	24.1	34.5	1.6	—
J1955+2908	jbo, nrt	157	8.1	6.5	6.1	117.35
J2010−1323	jbo, nrt	390	7.4	1.9	5.2	—
J2019+2425	jbo, nrt	130	9.1	9.6	3.9	76.51
J2033+1734	jbo, nrt	194	7.9	12.7	5.9	56.31
J2124−3358	jbo, nrt	544	9.4	3.2	4.9	—
J2145−0750	eff, jbo, nrt, wsrt	800	17.5	1.8	16.1	6.84
J2229+2643	eff, jbo, nrt	316	8.2	4.2	3.0	93.02
J2317+1439	eff, jbo, nrt, wsrt	555	17.3	2.4	3.4	2.46
J2322+2057	jbo, nrt	229	7.9	5.9	4.8	—

5 MSPs with rms under 1 μs

Results from the EPTA dataset 2015

Results on GWB, isotropic

(Lentati & EPTA collaboration accepted in MNRAS)

Model	95% upper limit
Stochastic GWB	
Fixed Noise - Fixed Spectral Index	1.7×10^{-15}
Varying Noise - Fixed Spectral Index	3.0×10^{-15}
Additional Common Signals - Fixed Spectral Index	3.0×10^{-15}
Fixed Noise - Varying Spectral Index	8×10^{-15}
Varying Noise - Varying Spectral Index	1.3×10^{-14}
Additional Common Signals - Varying Spectral Index	1.3×10^{-14}

Results on anisotropy shows consistency with isotropy

(Taylor & EPTA collaboration accepted in PRL)

Results from the EPTA dataset 2015

Results on Single Sources

(Babak & EPTA collaboration submitted to MNRAS)

Several Method have been used :

- Frequentist approach for non evolving sources
 (Ellis et al. 2012)
- Frequentist approach for evolving sources
 (Babak & Sesana 2012, Petiteau et al. 2013)
- Bayesian approach for evolving sources with full signal
 (Lassus et al. in prep.)
- Bayesian approach for evolving sources with Earth term only

- Bayesian approach for non evolving sources with phase marginalization
 (Taylor et al. 2014)

Results from the EPTA dataset 2015

Results on Single Sources

(Babak & EPTA collaboration submitted to MNRAS)

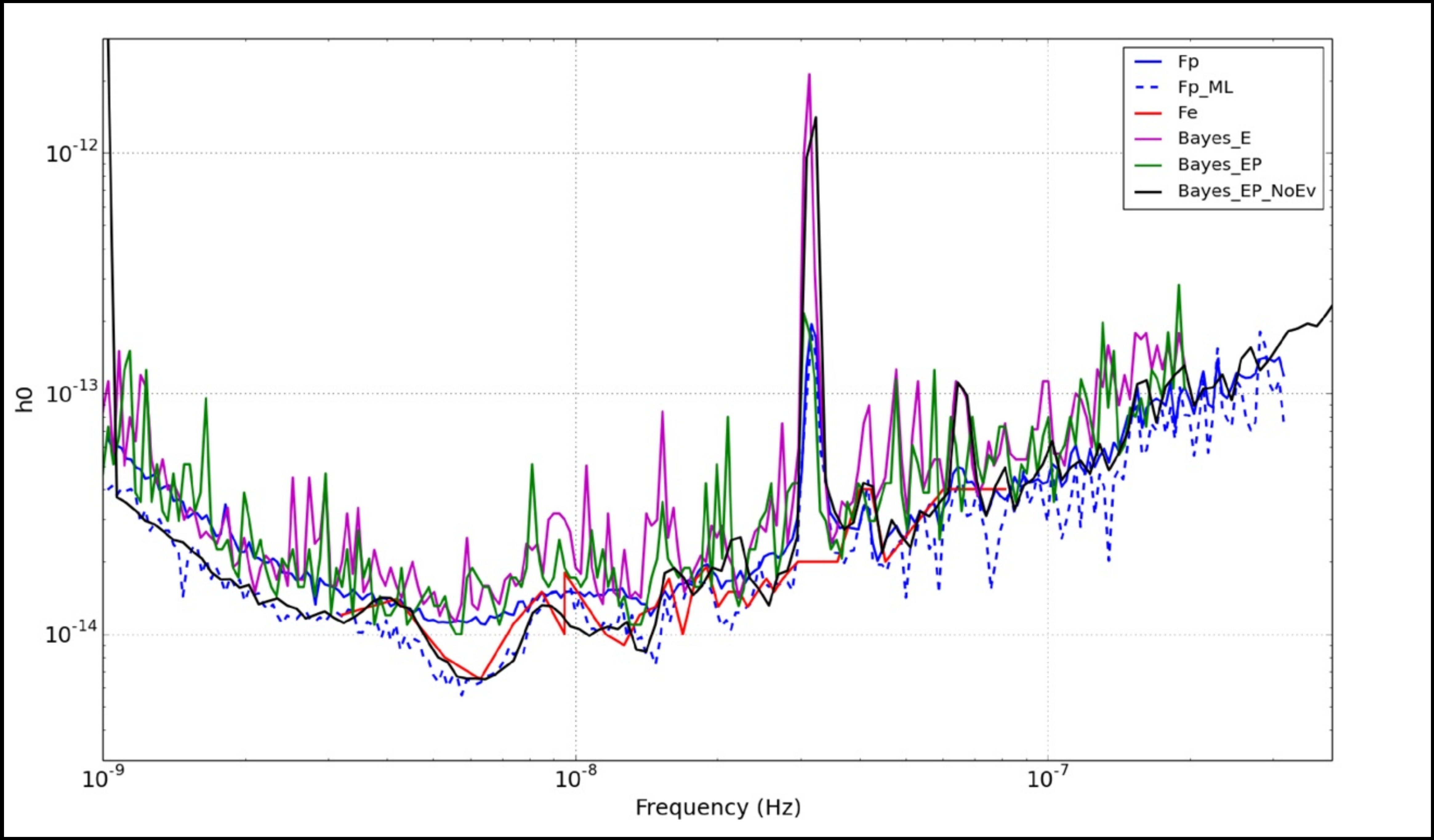

Results from the EPTA dataset 2015

Results on Single Sources

(Babak & EPTA collaboration submitted to MNRAS)

Sensitivity Sky Map for the frequentisit method with evolving sources at 6.3 nHz

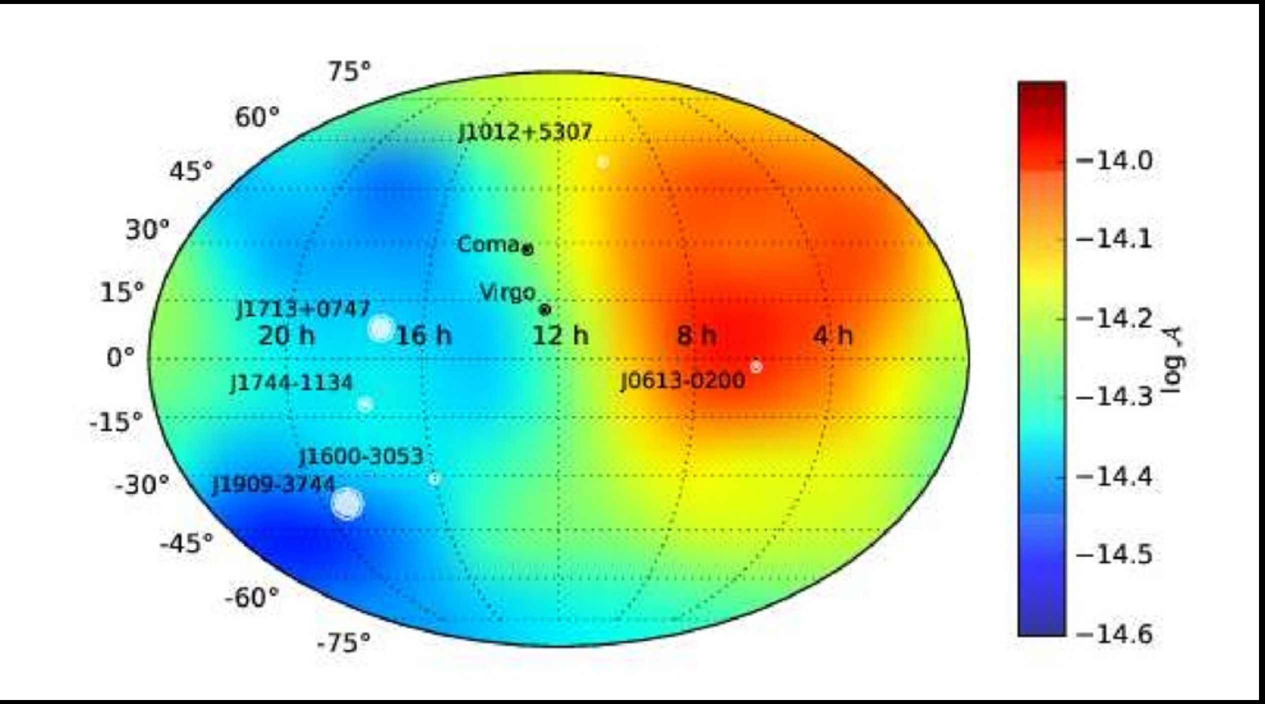

Sensitivity Sky Map for the bayesian method with non evolving sources at 7 nHz

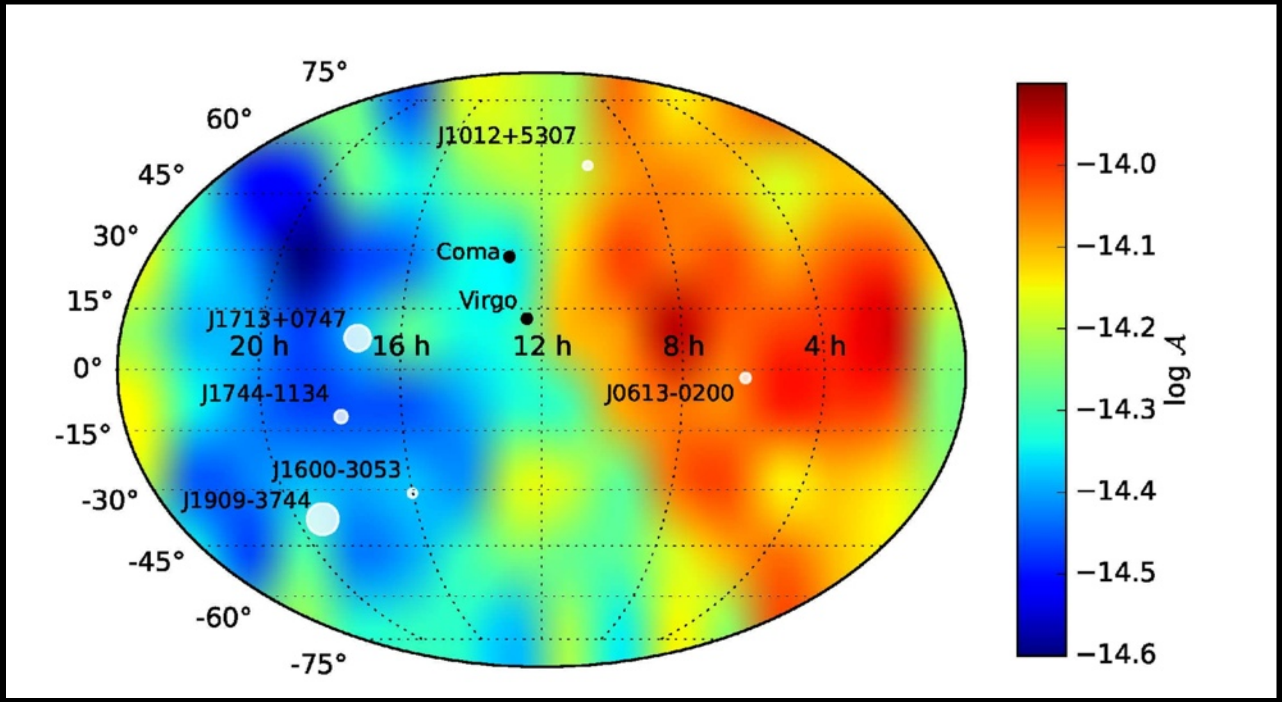

Results from the EPTA dataset 2015

Results on Single Sources

(Babak & EPTA collaboration submitted to MNRAS)

In the our best frequency interval (5-7 nHz) :

$$6 \times 10^{-15} < A_{95\%} < 1.2 \times 10^{-14}$$

We can exclude the presence of SMBHBs with separation < 0.01pc to a distance of 25Mpc (well beyond Virgo) for :

$$\mathcal{M}_c > 10^{9} \mathrm{M}_{\odot}$$

We can exclude the presence of SMBHBs with separation < 0.01pc to a distance of 25Mpc (twice the distance to Coma cluster) for :

$$\mathcal{M}_c > 10^{9.5} \mathrm{M}_{\odot}$$

Thank You !

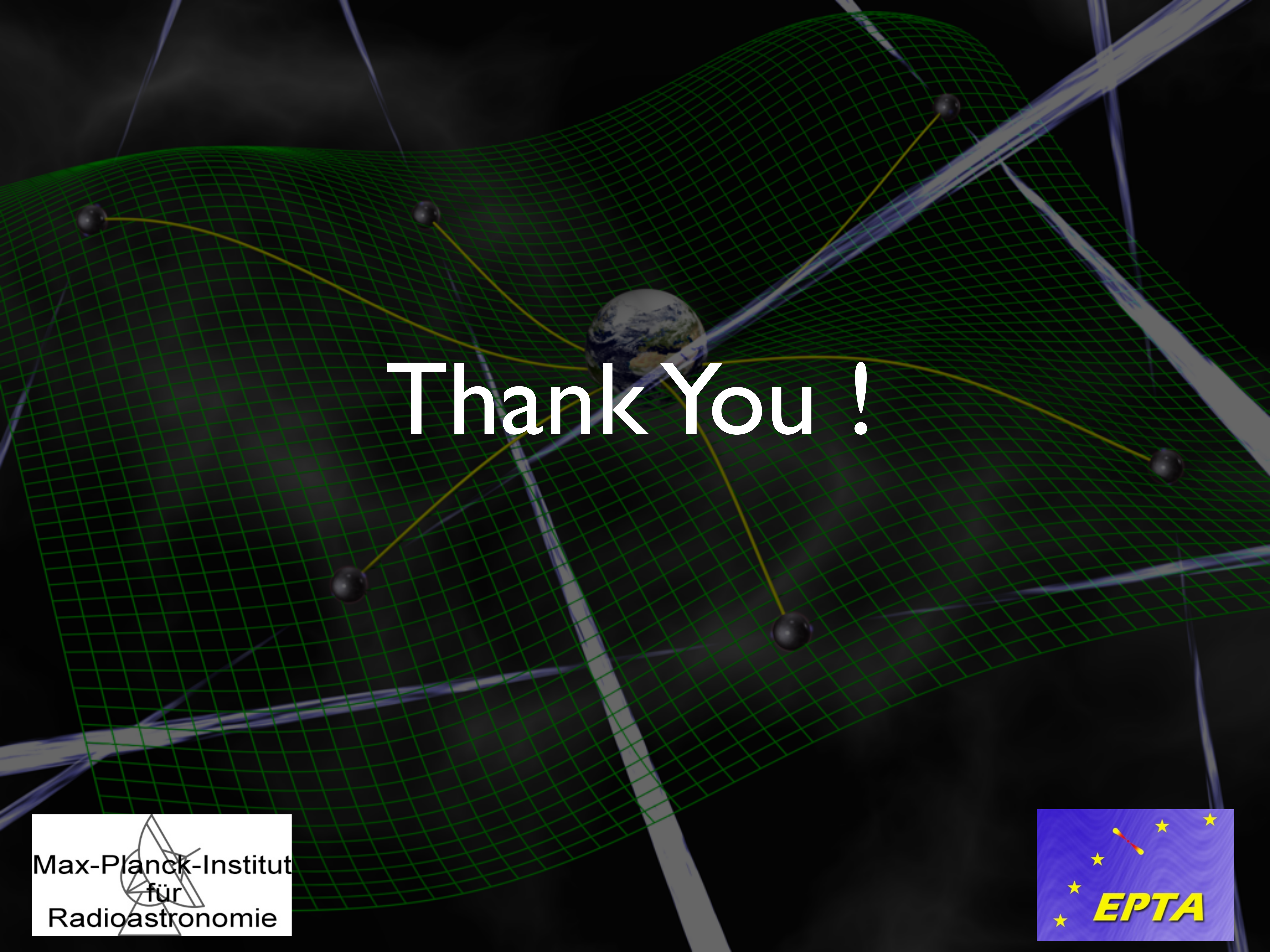

Max-Planck-Institut für Radioastronomie

EPTA